Description of *Carbo*-oxocarbons and Assessment of Exchange-Correlation Functionals for the DFT Description of *Carbo*-mers

Christine Lepetit,[†] Henry Chermette,*[,‡] Mickaël Gicquel,[†] Jean-Louis Heully,[§] and Remi Chauvin[†]

Laboratoire de Chimie de Coordination, UPR 8241 CNRS, 205 Route de Narbonne, 31 077 Toulouse Cedex 4, France, Laboratoire de Chimie-Physique Théorique, Université de Lyon, Université Lyon 1, and CNRS UMR 5182, Bât 210-Dirac, 43 Bd du 11 novembre 1918, F-69622 Villeurbanne Cedex, France, and Laboratoire de Physique Quantique, IRSAMC, UMR 5626-118, route de Narbonne, 31077 Toulouse Cedex 04, France

Received: June 29, 2006; In Final Form: October 6, 2006

Mono- and polycyclic valence isomers of *carbo*-[3]oxocarbon C_9O_3 and *carbo*-[5]oxocarbon $C_{15}O_5$ have been characterized on the singlet spin state potential energy surface. By contrast to their geometry, their relative stability is highly sensitive to the calculation level. The performance of LDA, GGA, *meta*-GGA, and hybrid functionals is compared to that of HF, post-HF, and multiconfigurational calculations. The results obtained for C_9O_3 are compared to those obtained for hydrocarbon analogues such as [3]pericyclyne $C_9(H_2)_3$ and *carbo*-[3]radialene $C_9(CH_2)_3$ and are analyzed on the basis of an energy decomposition scheme. The respective role of the exchange and correlation counterparts of the functional in the discrepancy of the results is discussed.

Introduction

In 1995, a novel partition of molecular structures, referred to as *carbo*-mers, was formally defined on the basis of a "carbon-enrichment" criterion.[1] Since then, exploratory computational studies have been performed on four series of ring *carbo*-mers of cyclic molecules (Scheme 1),[2] ranging from cycloalkanes,[3] [*n*]annulenes,[4] and "aromatic" heterocycles[5] to [3]radialenes.[6] The (homo)aromaticity of these structures has been thoroughly studied and characterized using classical aromaticity criteria, or criteria based on the electron localization function (ELF) analysis.[2] Synthetic targets have been suggested and potential applications, especially in nonlinear optics, have been pointed out.[7] Experimentally, several *carbo*-cycles such as functional pericyclynes and *carbo*-benzenes have been prepared.[8]

Carbo-[*n*]oxocarbons, the oxygenated analogues of *carbo*-[*n*]radialenes (Scheme 1), are the next natural targets in the series of cyclic *carbo*-mers. The parent molecules have been isolated only as dianions involved in complexes of alkali or transition metals.[9] Although *carbo*-[*n*]oxocarbons remain experimentally unknown, the influence of *carbo*-merization on the aromaticity, stability, reactivity, and coordination chemistry of the oxocarbons therefore deserved to be theoretically studied.[10,11]

Considering the large size of the *carbo*-[*n*]oxocarbons, a preliminary study of the first member of the series, i.e., *carbo*-[3]oxocarbon C_9O_3, aimed at calibrating the calculation method. Since the use of DFT methods cannot be circumvented for the calculation of the highest members of the series ($n > 3$), the first aim was thus to find the most suited functional for the description of *carbo*-[3]oxocarbon.

Two valence isomers of *carbo*-[3]oxocarbon C_9O_3, have been obtained on the singlet spin state potential energy surface. The monocyclic isomer **1a** is the ring *carbo*-mer of the neutral oxidized form of deltate, while the tetracyclic isomer **1b** is the trioxo derivative of tricyclopropabenzene (Scheme 2).[12] By contrast to their geometry, which is barely sensitive to the calculation level, the relative stability of **1a** and **1b** is highly sensitive to the calculation method used.

In this work, the performance of LDA, GGA, *meta*-GGA, and hybrid functionals is compared to that of HF, post-HF, and multiconfigurational calculations. The results are hereafter tentatively rationalized in terms of the respective role of the exchange and correlation counterparts of the functional in the decomposition of the relative energy of the valence isomers **1a** and **1b**. The results are also discussed in comparison with hydrocarbon analogues of *carbo*-[3]oxocarbon such as [3]-pericyclyne $C_9(H_2)_3$ and *carbo*-[3]radialene $C_9(CH_2)_3$.

The remainder of this paper is organized as follows: after a brief description of the computational details, the valence isomers **1a** and **1b** of *carbo*-[3]oxocarbon are introduced. Then, the relative energies of **1a** and **1b** obtained with a wide panel of DFT XC functionals are compared, and the characteristics and similarities of those providing significantly different results are analyzed. The next section deals with the sensitivity to the calculation level of hydrocarbon analogues of **1**. The size effect is then illustrated by considering *carbo*-[5]oxocarbon **4**. Quadrupolar effects are discussed in the next section. Then, an analysis of the respective contributions of the exchange and correlation energies in all classes of compounds is proposed. The last section focuses on an energy decomposition analysis of the C_9O_3 isomers **1a** and **1b** in comparison with the corresponding C_3O fragments. A short conclusion closes the paper.

Computational Details

Geometries were fully optimized under symmetry constraint whenever possible at various theory levels using the Gaussian03 code and the 6-311+G* basis set,[13] or the ADF2005.01 code

---

* Corresponding authors. E-mail: henry.chermette@univ-lyon1.fr.

[†] UPR 8241 CNRS.

[‡] Université de Lyon, Université Lyon 1 and CNRS UMR 5182.

[§] IRSAMC.

10.1021/jp064066d CCC: $37.00

SCHEME 1: Various Series of Ring *Carbo*-mers

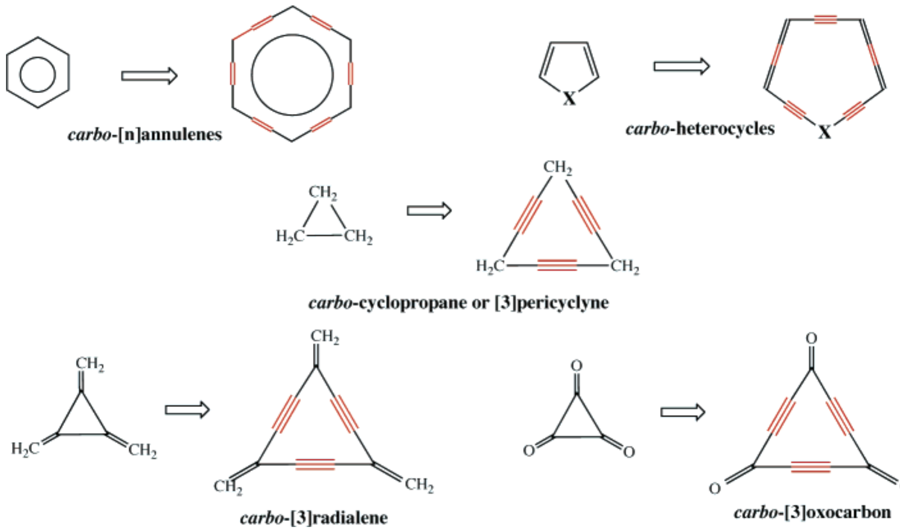

SCHEME 2: Most Representative Resonance Forms of the Valence Isomers 1a and 1b of C_9O_3

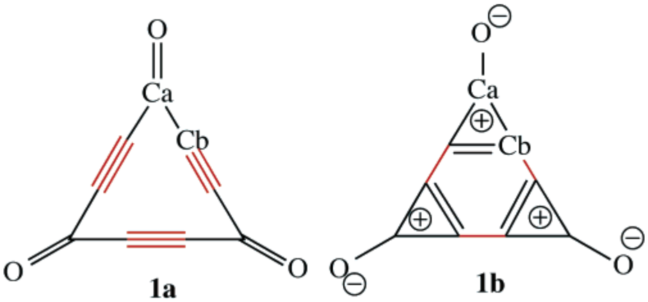

1a **1b**

and the TZP basis set.[14] Vibrational analysis was performed at the same level as the geometry optimization in order to check if true minima were obtained on the potential energy surfaces. Frontier orbitals contours were drawn with the Molekel visualization package.[15] The Self-Interaction-Corrected calculations have been performed with a modified version of the ADF2004.01 code.[14] CCSD geometry optimizations were performed with the NWChem 4.6 code,[16] using the 5-31G* basis set extracted from GAMESS.[17]

Results and Discussion

1. Presentation of the *Carbo*-oxocarbons. The *carbo*-[*n*]-oxocarbons are appealing structures for the study of the influence of *carbo*-merization on the aromaticity, stability, reactivity, and coordination chemistry of parent molecules, namely [*n*]oxocarbons (Scheme 1). The latter have indeed been isolated only as aromatic dianions exhibiting versatile coordinating properties.[9]

Experimentally, *carbo*-[*n*]oxocarbons might be accessible by oxidation of *n*-hydroxy-[*n*]pericyclynes. A complete retrosynthesis of the first member of the series, *carbo*-[3]oxocarbon **1a** (Scheme 3) is supported by the previously established general reactivity of starting materials to be coupled, i.e., 1,4-pentadiyn-3-ol and the cobalt complex of butyndial (otherwise intrisinsically instable).[18] A longer but similar strategy can be devised for *carbo*-[5]oxocarbon **4a** (Scheme 4).[18b]

The computational studies focused also first on the first member of the series, i.e., *carbo*-[3]oxocarbon **1**. The calibration of the calculation method that will be described here aims at studying the sensitivity of the structure of **1** to the calculation level. Moreover, these computational studies allowed derivation of the geometry, the electronic structures, and the aromatic properties of *carbo*-[3]oxocarbon and of its isomers. Possible interconversion pathways between isomers have been also studied. These results will be reported in details elsewhere.[11]

At the B3PW91/6-311+G* level of calculation, two valence isomers of D_{3h} symmetry of C_9O_3 have been obtained on the singlet spin state potential energy surface. *Carbo*-[3]oxocarbon (**1a**) is a monocyclic isomer involving a C_9 ring, whereas a tetracyclic isomer (**1b**) is made of three peripheral cyclopropenone rings annelating a central cyclohexatriene ring (Figure 1).

The tetracyclic form **1b** is 33.1 kJ/mol less stable than the monocyclic form **1a**. This energy gap is much smaller than the corresponding values of 204.4 and 156.8 kJ/mol obtained at the same level for the hydrocarbon analogues $C_{12}H_6$ (**2**) and C_9H_6 (**3**) respectively (Scheme 4). At first sight, this specific stabilization may be ascribed to the aromaticity of the three cyclopropenone rings of **1b** (induced by the natural polarization of the carbonyl groups $C{=}O \leftrightarrow C^{+}{-}O^{-}$). A possible partial aromaticity of the central six-membered ring might also be invoked. The calculated monocyclic structures of *carbo*-[3]-radialene (**2a**) and [3]pericyclyne (**3a**) are reported elsewhere.[2,3,6,12,19]

2. Sensitivity of the Relative Energy of 1a and 1b to the Calculation Method.

2.1. Results. The D_{3h} structure of **1a** and **1b** was investigated at various levels of theory. The geometry of both isomers appears to be slightly sensitive to the calculation level (Tables S1 and S2). Hybrid functionals (HDFT) yield comparable geometries, slightly different from MP2 and GGA geometries, with a quite good overall agreement between them. *Trans*-annular Cb−Cb bonds and endocyclic Cb−Cb bonds of isomer **1b** (Scheme 2) are calculated to be shorter at the HDFT levels.

Concerning the electronic structure of each isomer, three classes of calculation methods may be distinguished: HDFT, GGA, and HF/MP2 (Tables S1 and S2), The HOMO−LUMO gap is the same within a given class of methods and increases from GGA to HF/MP2 estimates, as expected.[20,21] The electronic configuration is also the same within each class and is consistently modified from GGA to HF/MP2 *via* HDFT calculations. Indeed, the less the amount of exact exchange, the more the π_z orbitals are stabilized (Figure S1). This is in agreement with the fact that DFT calculations have been shown to overestimate electron delocalization whereas HF calculations underestimate it.[22]

SCHEME 3: Proposed Retrosynthesis of *Carbo*-[3]oxocarbon

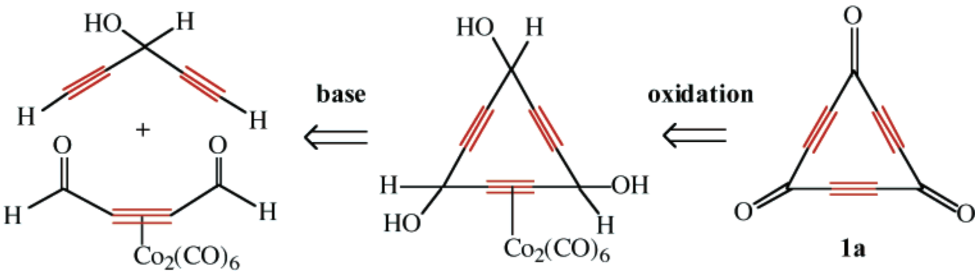

SCHEME 4: Most Representative Resonance Forms of the Valence Isomers of [3]pericyclyne 2 ($C_9(H_2)_3$), *Carbo*-[3]radialene 3 ($C_9(CH_2)_3$), and *Carbo*-[5]oxocarbon 4 ($C_{15}O_5$)

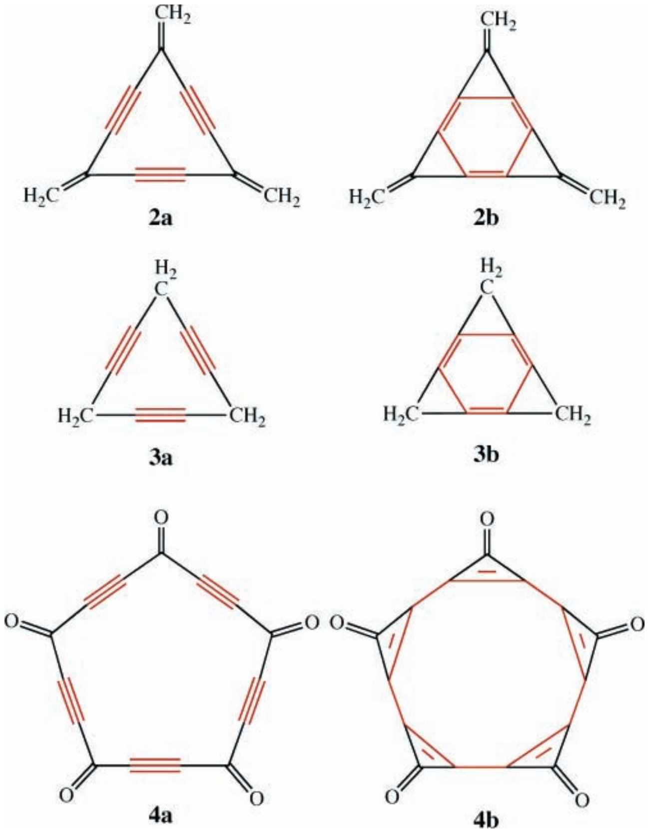

By contrast to the structural results, the relative stability of **1a** and **1b** is highly sensitive to the calculation level (Table 1). HF, post-HF methods, BLYP, and B3LYP yield a comparable energy gap close to 100 kJ/mol. GGA functionals other than BLYP estimate this energy gap to be about 50 kJ/mol, whereas the lowest values of about 30 kJ/mol are obtained using HDFT functionals other than B3LYP. These first results suggest that the correlation part of the functional may be at the origin of the discrepancy in the results.

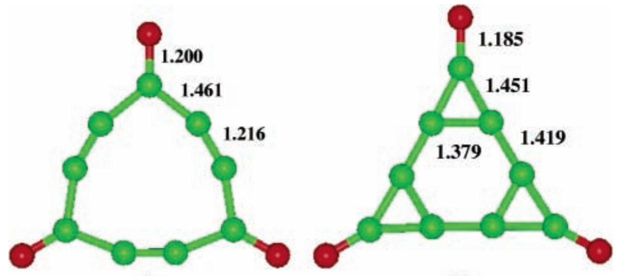

1a **1b**

Figure 1. Calculated structures (B3PW91/6-311+G*) of the isomers **1a** and **1b** of C_9O_3. Distances are in angstroms.

As no related compounds have been yet isolated, calculations of higher level were used as a standard. Single point CCSD//B3PW91 calculations are in agreement with the above B3LYP or MP2 results (Table 1). However, the corresponding T_1 diagnostic value of 0.018 is close to the acceptable highest limit of 0.02[23] and suggests that multireference calculations may be required. A rough CASSCF analysis on a limited active space ruled out this hypothesis. Finally, geometry optimization of isomers **1a** and **1b** was achieved at the CCSD/5-31G* level. **1a** is found to be 115.4 kJ/mol higher in energy than **1b**. This relative energy is in good agreement with the above single point CCSD//B3PW91 calculations and lies in the range of the above B3LYP or MP2 results (Table 1). The small geometrical deviations observed at the CCSD/5-31G* level of calculation may be assigned to a basis effect. Post-HF methods are indeed known to be much more basis set sensitive than DFT methods.

Facing the scattering of the DFT description of *carbo*-oxocarbons (Table 1), we examined the performance of a larger set of XC functionals. For this purpose, the ADF code was used.[14] For a given XC potential, it allows for the direct calculation of the energies belonging to a wide panel of combinations of exchange and correlation energy functionals. More precisely, a group of 58 functionals belonging to LDA, GGA, HDFT or *meta*-GGA DFT generations, were tested (see the table in the Appendix). The energy gap between isomer **1a** and **1b** was estimated from single point calculations performed on geometries obtained at the B3PW91, PBE, or MP2 level. It should be noted that the results are little dependent on the level of theory or on the nature of the XC functional used for the geometry optimization. The great similitude of the potential energy surfaces of a given system calculated with different exchange-correlation functionals has been noted recently.[29]

The energy gaps between isomers **1a** and **1b** shown in Figure 2 seem much more scattered than those given in Table 1, although the first-evidenced tendencies remain valid: most of the functionals belonging to a given category (GGA, hybrid) do provide very similar results.

2.2. Characteristics of Poor-Performing Functionals. Assuming that the CCSD calculations are reliable, seven functionals predict the wrong relative stability order of isomers **1a** and **1b**. These cases are examined below.

(i) LDA. It is currently admitted that LDA underestimates exchange by more than 10−14%, whereas it overestimates correlation (which is 1 order of magnitude smaller) by 100−150%. In most cases, their combination thus lead to reasonable energies, but still overestimates bond energies. Here, because small energy differences are at stake, the LDA is not sufficiently accurate. Indeed, as discussed hereafter, the correlation counterpart here plays a dominant role, indicating that the dynamical correlation in these delocalized π-systems is substantial. The importance of the exchange functional should not be neglected

TABLE 1: Energy Gap between Isomers 1a and 1b Obtained at Various Levels of Calculations (6-311+G* Basis Set). Second Row of the Table Shows the Zero-Point Energy (ZPE) Corrected Values

energy (kJ/ mol)	B3PW91	B3P86	PBE0	B97-2	BP86	BPW91	PBE	BLYP	B3LYP	MP2	CCSD//B3PW91	HF
Δ*E* **1b** vs **1a**	33.1	36.3	15.3	21.6	50.7	40.4	31. 2	110.8	91.7	106. 0	126.1	120. 7
Δ*E* (ZPE corr.)	36.1	39.3	18.6	25.2	53.4	43.2	34. 4	112.4	93.8	112. 6	-	121. 9

either, because it contains the static (quasidegeneracy) correlation,[24,25] which also seems important for these highly symmetrical systems.

(ii) OPTX Exchange. In the case of OPBE, OPBE0, and OP86 combinations, the OPTX exchange[25] part is responsible for predicting the wrong relative stability order of isomers **1a** and **1b**. This functional has been parametrized to reproduce Hartree−Fock exchange for atoms, but its authors did argue that such a functional contains static (i.e., left-right, nondynamic, or near-degeneracy) correlation. Its local component, i.e., at zero (reduced) density gradient, is close to the Xα functional. The latter differs from the Dirac−Slater exchange (exact for electron gas) by a factor which has been taken in the past either as an atom-dependent constant (in the early MS-Xα method)[26] or a global constant near to $0.7/(2/3) = 1.05$. The standard 0.7 coefficient of the Slater exchange is the value retained in the so-called Hartree−Fock−Slater LCAO code and its variants, such as the DVXα codes in the seventies,[27] and, at present, the ADF code in case of the default α value for the Xα functional. The 2/3 value is the theoretical value for the electron uniform gas. For large density gradients, the OPTX exchange functional is supposed to be quite close to most other GGAs (through an enhancement factor similar to that of most GGAs for medium or large gradients). More precisely, in OPTX, the reduced gradient enters in a power of 4 in the Ex expression, whereas most other GGAs use a power of 2. An exception is the B97 exchange functional which uses both powers of 2 and 4. Grüning and Baerends emphasized this difference as mainly responsible for the quite different performance (generally better) of OPTX as compared to B88 or PW91, as far as thermochemistry of G2,G3 type database is concerned.[28] The choice of the OPTX exchange functional as component of a XC functional (GGA or hybrid), which appeared to be very satisfactory for many purposes, also led to significantly biased properties or energy differences in some classes of compounds.[29] In the present case, this functional overstabilizes the polycyclic structures like **1b** *versus* **1a**.

(iii) VSXC and B00 *meta*-GGAs. The case of VS98, sometimes denoted as VSXC by their promoters,[30] can be traced back to its elaboration scheme: although this functional contains several appealing physical features, it was obtained through a fit of 21 parameters against a data basis (an extension of the G2 data base[31]) containing mostly very small systems. A great number of parameters may produce spurious compensations of errors hidden for the majority of systems. Whereas it is very efficient for the description of "classical" molecules, it may be less accurate for more "exotic" molecules. Moreover, this functional is known to overestimate long-range bonding effects such as hydrogen bonding or $\pi-\pi$ stacking. Indeed, some dramatic failure of this functional for describing torsion potentials in π-conjugated systems has been demonstrated.[32] Interestingly, here, VS98 lets us describe our π-conjugated systems in a way intermediate between standard GGAs and GGAs with LYP. The relative contributions of the correlation and exchange counterparts are however different from what it is for the majority of the XC functionals (*vide infra*).

Some combinations involving an exchange part extracted from an exchange-correlation functional elaborated through a simultaneous optimization of both (exchange and correlation) counterparts may lead to spurious results: this is the case of the B00 exchange functional,[33] derived from a model aiming at an improved description of atomic hydrogen, delocalized systems, or systems with a small number of electrons instead of the electron gas, and this functional should not be used

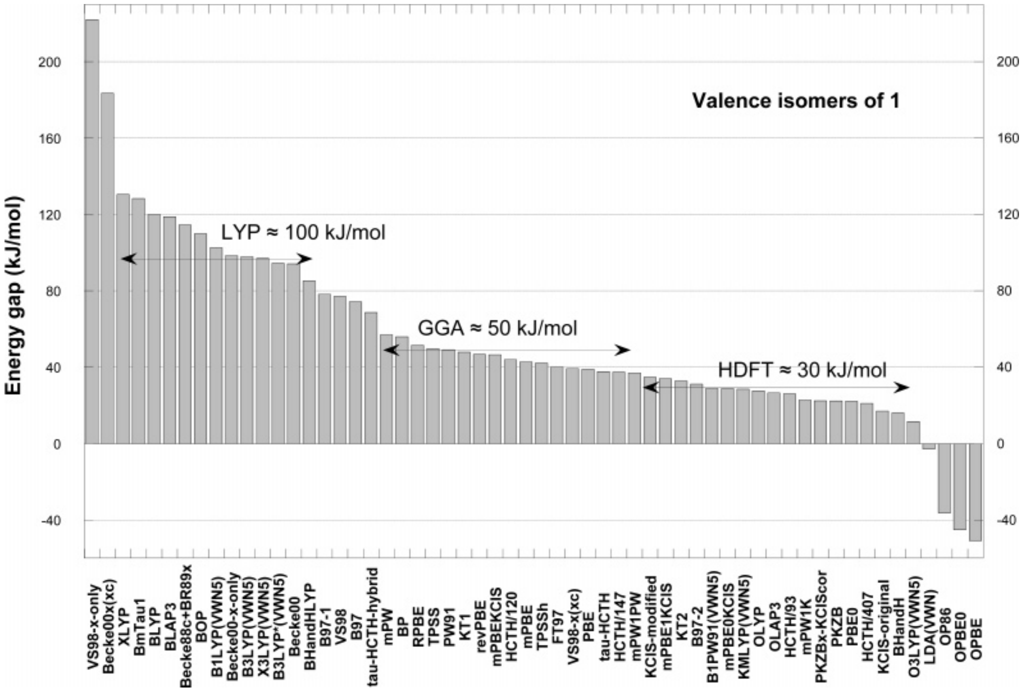

Figure 2. Relative energy (kJ/mol) between isomers **1a** and **1b** obtained at various levels of calculations. Geometries were optimized at the B3PW91/6-311+G* level.

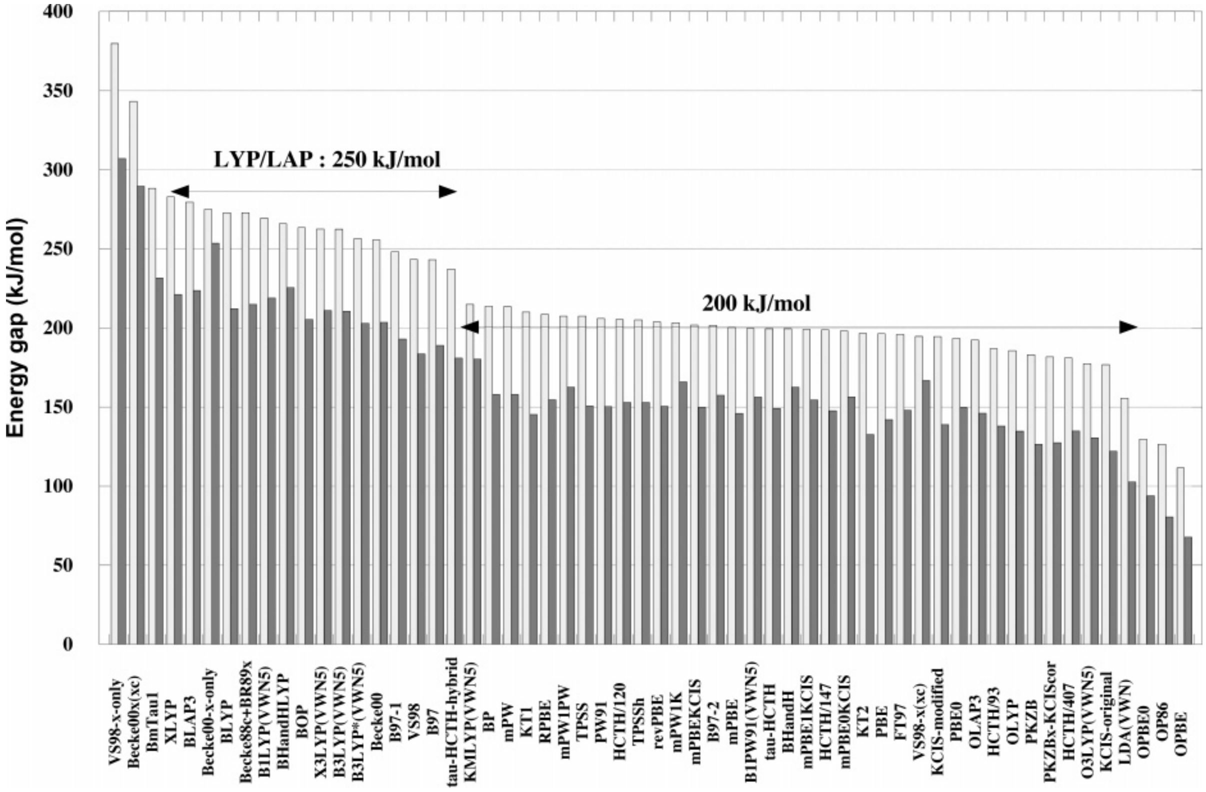

Figure 3. Energy gap between monocyclic and tetracyclic isomers of **2** (white bars) and **3** (dark gray bars) obtained at various levels of calculations. Geometries were optimized at the B3PW91/6-311+G* level.

TABLE 2: Energy Gap (kJ/mol) between Monocyclic and Polycyclic Isomers of Compounds 1−3 and Corresponding ZPE-Corrected Values, Obtained at Various Levels of Calculations (6-311+G* Basis Set)

compound	B3PW91	B3LYP	MP2
C_9O_3 (**1**)	33.4	91.5	105.8
corr. ZPE	36.0	93.6	112.4
C_9H_6 (**2**)	156.8	208.2	218.6
corr. ZPE	154.7	204.8	216.9
$C_{12}H_6$ (**3**)	204.4	260.4	279.6
corr. ZPE	201.9	256.7	277.1

without its correlation counterpart. Outliers such as VS98-x-only, VS98-x(xc), and Becke00x(xc) fall in this category.

2.3. Characteristics of Well-Performing Functionals. In reference to CCSD calculations, the functionals involving a LYP or Lap correlation part performs quite well. By contrast to the OPTX exchange functional, the LYP correlation strongly favors structure **1a** with respect to **1b** for every XC functional it belongs to. This feature is somehow weakened in a few hybrid functionals in which the LYP is weighted by a factor smaller than 1 (e.g., B3LYP contains only 81% of LYP). This is clearly apparent in Figure 2. When LYP is coupled to OPTX, some cancelation of errors tends to annihilate the deviation from the LDA results, and this will also be the case in the O3LYP hybrid functional. At the O3LYP level, **1a** and **1b** are indeed almost degenerate as they are at the LDA level. This underlines the fact that in such π-conjugated systems, the role of the dynamic correlation may be prominent.

LYP is a restatement of the correlation-energy formula of Colle and Salvetti in terms of density and kinetic energy density.[34] Using a second-order gradient expansion for the kinetic energy density, and retaining the Colle−Salvetti param-

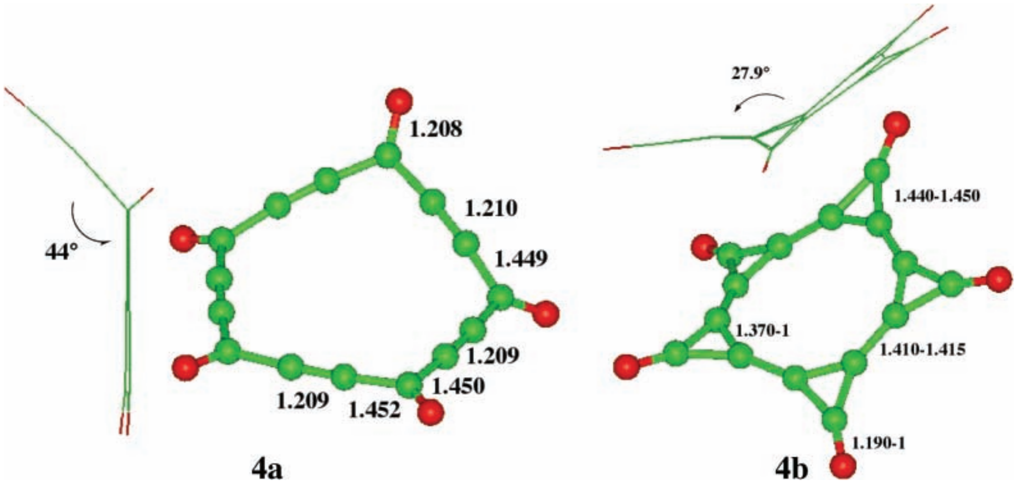

Figure 4. Calculated structures (B3PW91/6-311+G*) of isomer **4a** and **4b** of $C_{15}O_5$. Distances are in angstroms.

TABLE 3: Energy Gap (kJ/mol) between Monocyclic and Polycyclic Isomers of 4 and Corresponding ZPE-Corrected Values, Obtained at Various Levels of Calculations (6-311+G* Basis Set)

compound	B3PW91	B3LYP	MP2
$C_{15}0_5$	−38.5	60.6	102.8
corr. ZPE	−32.6	64.0	-[a]

[a] Because of the high computational cost, the vibrational analysis of **4** was not available at this level, but minima of comparable geometry were found at the MP2/6-31+G* level for which the energy gap is 82.3 kJ/mol.

eters fitted to the Hartree−Fock orbitals of helium, LYP has become one of the best performing correlation energy functionals. However, it does not contain parallel spin contribution to correlation. The "one-parameter progressive" OP correlation functional developed by Tsuneda, Suzumura, and Hirao[35] is also derived from the Colle−Salvetti correlation functional and, coupled to Becke88 exchange, it leads to results lying in the same range.

Lap is a τ- and Laplacian-dependent correlation functional that has been developed by Proynov et al. by explicitly solving the adiabatic connection formula with model pair correlation functions.[36,37] It has been coupled to Becke88 exchange or Perdew-Wang86 exchange functional in the BLap and PLap XC functionals, respectively, and later on, the Bmτ1.[38] The data set used for the optimization contained a set of small molecules but also the water dimer. The τ1 correlation functional contains a parallel spin contribution which requires a reoptimization of the exchange functional to which it is coupled. These functionals do provide results closer to LYP than to the KCIS family, probably also because of the databases used for the optimization of their respective parameters. This situation is quite different from the Perdew86, Perdew-Wang91, PBE, or TPSS correlation functionals which have been derived from the electron gas model and perform generally better for extended systems than for localized systems. In a recent work,[39] it has been shown that the TPSS correlation plays a minor role in the description of π systems.

2.4. The Three Main Classes of Functionals. As compared to the CCSD calculations, most of the other functionals predict the right relative stability order of isomers **1a** and **1b**, and again three ranges of energy gap may now be distinguished:

(i) 18 functionals estimate an energy gap lying in a satisfactory range 68.7 kJ/ mol (τ-HCTH-hybrid) to 130 kJ/mol (XLYP). Most of them involve a LYP or Lap correlation part. Considering the hybrid type functionals, the energy gap decreases according to the following order: BHandHLYP < B3LYP* < X3LYP ≈ B3LYP < B1LYP. At first glance, one could think that exact exchange tends to counterbalance the stabilization of **1a** resulting from the LYP correlation part: indeed this counterbalance comes from the reduced amount of the LYP correlation introduced in hybrid functionals. For instance the BLYP → B3LYP, B3LYP* is more affected by the change in LYP amount (100% → 81%) than the insertion of true exchange (15% in B3LYP*, 20% in B3LYP), coupled to a decrease of Becke88 GGA exchange (100% → 72%). A similar trend is found for XLYP → X3LYP and OLYP → O3LYP (these last functionals belonging to the following group, *vide infra*). The dominant role of the correlation part is demonstrated by the suitable result given by GGA functionals such as BLYP and XLYP.

(ii) 16 functionals, mainly GGA and most of the *meta*-GGA, estimate an energy gap lying in the lower range 37 kJ/mol (mPW1PW) to 57.1 kJ/mol (mPW), namely underestimated by a factor of 2. As expected, the GGA functionals of Table 1 fall in this range.

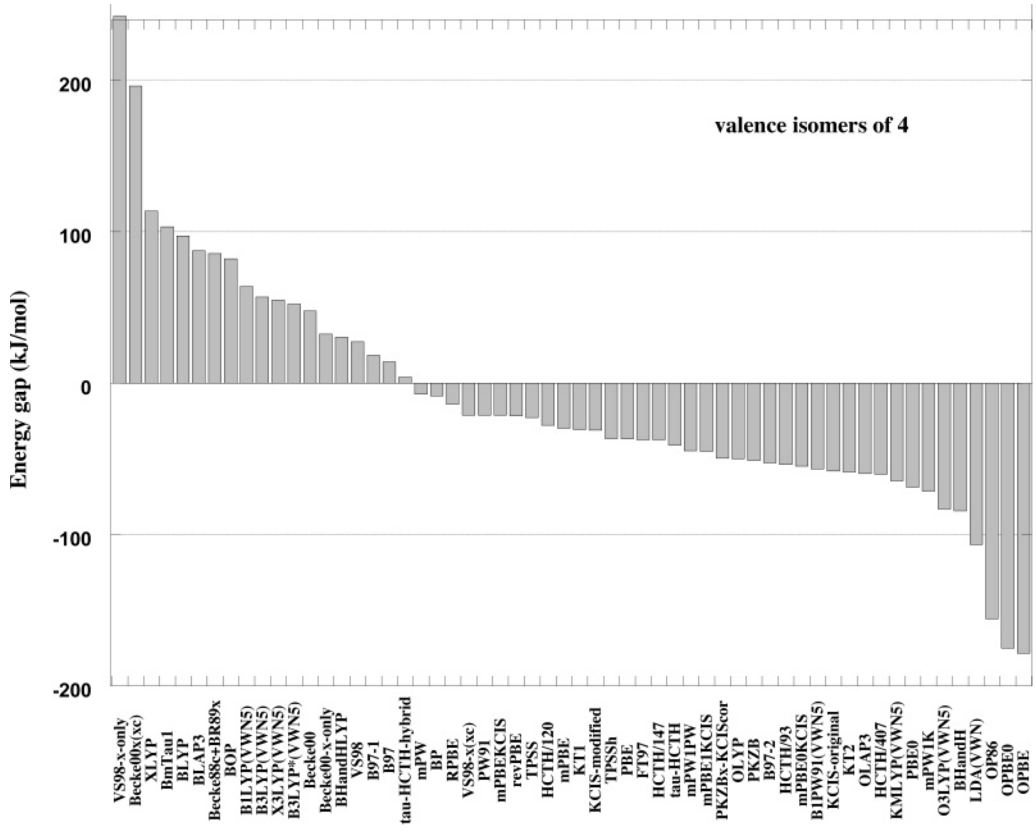

Figure 5. Energy gap between **4a** and **4b** obtained at various levels of calculation. Geometries were optimized at the B3PW91/6-311+G* level.

SCHEME 5: Fragmentation of Valence Isomers 1a and 1b into Linear and Cyclic C_3O Moieties

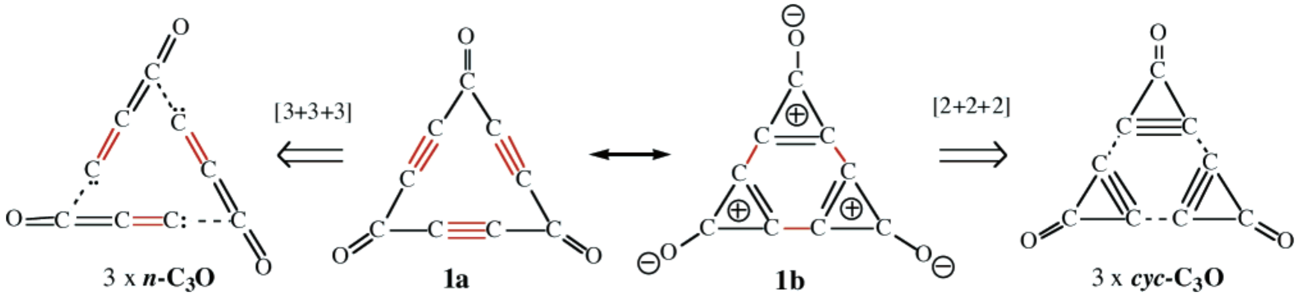

(iii) 17 functionals estimate an energy gap lying in a much lower range 16 kJ/ mol (BHandH) to 34.7 kJ/mol (KCIS-modified). Functionals of this class combine a correlation part other than LYP and/or an exchange part other than OPTX, in agreement with the previous findings. Half of them are HDFT. Finally, whereas LDA gives nearly degenerate isomers, GGAs with OPTX exchange decrease to a range near −40 kJ/mol.

It should be noted that successive reparametrizations of GGAs and *meta*-GGAs are not always successful: B97[40] and B97-1 yield similar gaps, but B97-2 underestimates the energy gap by a factor of 2; on the other hand, PBE, revPBE, and RPBE results do not differ significantly.

Calculations have been performed using the average density self-interaction correction (ADSIC) model recently proposed for molecular systems.[41−43] Whereas the geometry is different from that obtained with the crude functional, the energy gap is slightly lowered from 0.6 (respectively 43.2) kJ/mol to 0.36 (respectively 33.7) kJ/mol at the LDA (respectively PBE) level but remains of the same order of magnitude. This is not too surprising since the correction applies to both the Coulomb and the exchange terms, but not to the correlation (e.g., LYP is already self-interaction free).

3. Valence Isomers of Carbo-[3]radialene and [3]pericyclyne. The energy gaps between monocyclic and polycyclic isomers of hydrocarbon analogues of **1** were also calculated at various levels. The results are gathered in Table 2.

The calculation methods predict the same relative stability order. Again, B3LYP and MP2 results are very close and suggest that nine-membered ring based structures are much more stable than the corresponding tetracyclic geometries for hydrocarbon structures.

The performance of the previous set of 58 functionals was also examined for compounds **2** and **3**. In this case, the methods are in relatively good agreement, indicating that the monocyclic structure is much more stable than the tetracyclic one (Figure 3). However, functionals constructed with a LYP or Lap correlation part predict an increased stability of the monocyclic structure by about 50 kJ/mol with respect to other GGAs or *meta*-GGAs. Again, the XC functionals built with OPTX exchange predict a decreased stability of the monocyclic structure.

These results suggest that sensitivity of the description of **1** to the calculation method may be ascribed to the presence of heteroatoms and to C−O bonds more specifically.

4. Size Effect: Comparison with Valence Isomers of Carbo-[5]oxocarbon. Similarly to C_9O_3, two valence isomers of C_1 symmetry (far from planarity) have been obtained on the singlet spin state potential energy surface of $C_{15}O_5$ (Figure 4). *Carbo*-[5]oxocarbon (**4a**) is a monocyclic isomer involving a C_{15} ring whereas a polycyclic isomer (**4b**) is made of five peripheral cyclopropenone rings annelating a central nonplanar [10]-annulene ring. **4a** exhibits an envelope conformation with a folding angle of 44° of the tip, whereas in **4b** the tip is slightly less bent (about 30°). The geometry of the central [10]-annulene ring deviates substantially from those reported for hydrocarbon analogues.[44]

By contrast to C_9O_3, the polycyclic isomer is now 38.5 kJ/mol more stable than the monocyclic one at the B3PW91/6-311+G* level of calculation. The relative energy between monocyclic and polycyclic isomers of **4** were further calculated at various levels (Table 3). The comparable performance of B3LYP and MP2 noticed above upon analysis of the C_9O_3 findings appears to be fortuitous as the relative energy of isomers of **4a** and **4b** is now twice as large at the MP2 level as compared to the B3LYP level. Furthermore, the relative stability order is now method dependent. Indeed B3PW91 calculations predict the reverse stability order as compared to B3LYP or MP2 calculations (Table 3).

By contrast to **1**, the performance of the 58 functionals set was much more scattered for **4** (Figure 5). GGA (respectively HDFT) functionals with a non-LYP correlation part indicate that the polycyclic valence isomer **4b** is more stable by about 20 kJ/mol (respectively 55 kJ/mol), whereas the functionals with a LYP or Lap correlation part indicate the reverse stability order.

5. Quadrupolar Effects. The quadrupole moments of the valence isomers **a** and **b**, calculated at various levels of theory, have been compared for compounds **1**−**4** (Table S3). The magnitude of the components of the diagonal tensor is slightly lower for the monocyclic isomers **a** as compared to the corresponding polycyclic **b** isomers of compounds **1**, **2**, and **4** (it is however the reverse for compounds **3**). As it is more visible from the isotropic constant or from the norm of the vector, the shift is slightly larger in MP2 calculations but rather constant in DFT calculations. Due to the absence of dispersion in DFT methods, this would result in some understabilization of **b**-type isomers as compared to **a**-type isomers of compounds **1**, **2**, and **4** (the reverse for the pericyclyne series **3**). However, the difference in magnitude of the quadrupole moment (lower than 5% for **1**, **2**, **3**, and lower than 8% for **4**) does not appear to be significant enough to account for the large scattering of the **a/b** gaps. Quadrupolar effects may therefore be ruled out.

6. Correlation and Exchange Energy Analysis. As it is well-known, the balance between the exchange and the correlation energy contributions to the XC energy may vary from one XC functional to another. When a given functional is reparametrized, this balance may change according to the different properties and references of the training set used in the optimization. It is interesting to compare in this vein the correlation energy difference ΔEc between **1a** and **1b** (respectively **4a** and **4b**) which is presented in Figure 6a (respectively Figure 6b). It is apparent that ΔEc obtained with functionals constructed with Lap or LYP is about half the one obtained with other functionals, the two *meta*-GGAs VS98 and τ-HCTH being excepted. The functionals constructed with Lap or LYP thus favor the

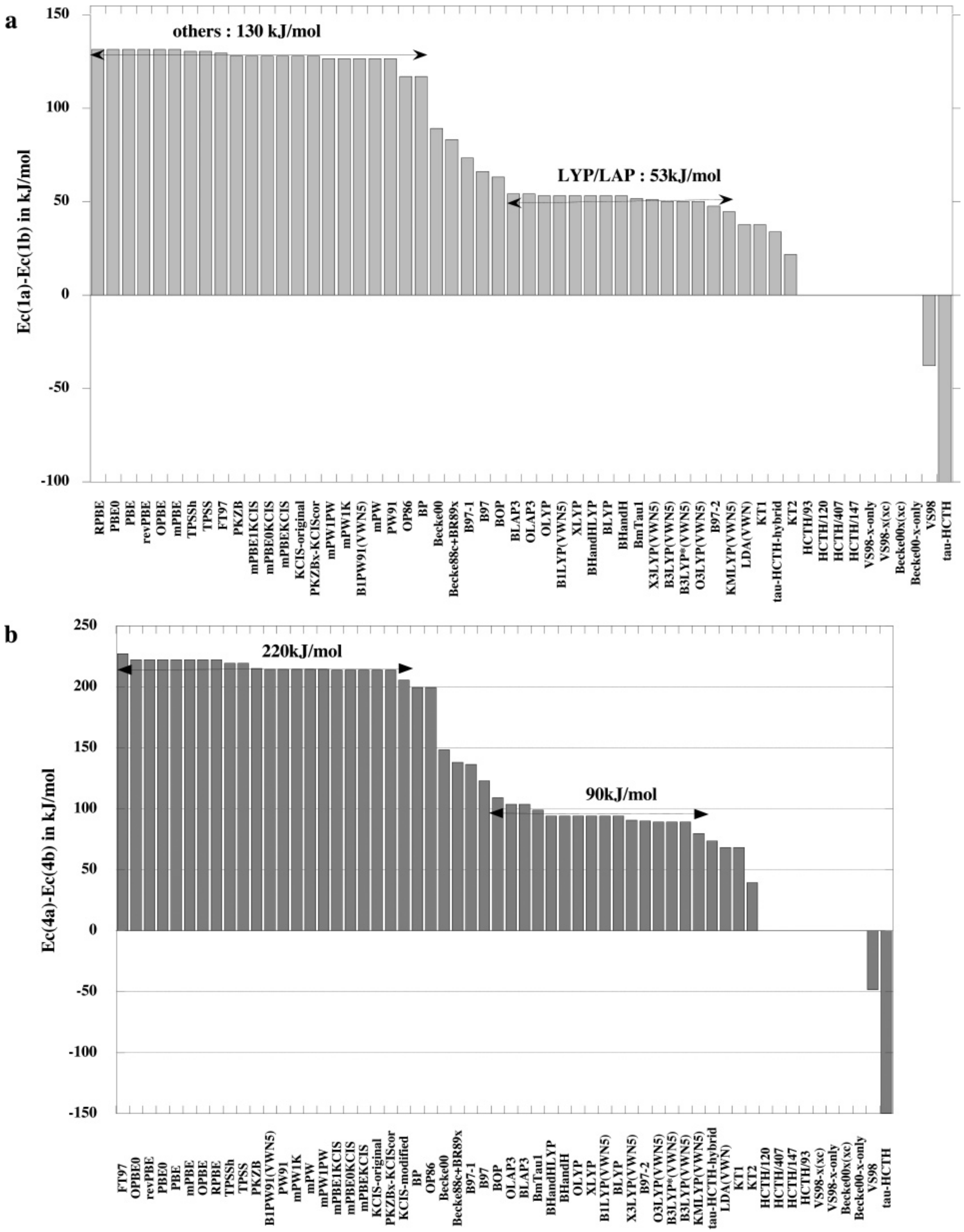

Figure 6. (a) Correlation energy gap between valence isomers **1a** and **1b**. (b) Correlation energy gap between valence isomers **4a** and **4b**.

monocyclic isomers **1a** and **4a**. It may be related to the method of elaboration of these correlation functionals, as mentioned previously (*vide supra*).

Compounds **1** and **4** may be considered as three, respectively five, C_3O fragments linked together. More specifically, **1a** (respectively **1b)** may be considered as a set of three "linear" (respectively cyclic) C_3O interacting fragments (Scheme 5). It is indeed apparent in Figure 6a (respectively Figure 6b), that the correlation energy difference ΔEc between **1a** and **1b** (respectively **4a** and **4b**) is about three (respectively five) times a value that might be related to the correlation energy difference between linear and cyclic C_3O fragments, i.e., about 18 kJ/mol for LYP/Lap based functionals and about 44 kJ/ mol for the others.

The relative stability of the hydrogenated representatives of these fragments (H_2C_3O), namely propynal and cyclopropenone,

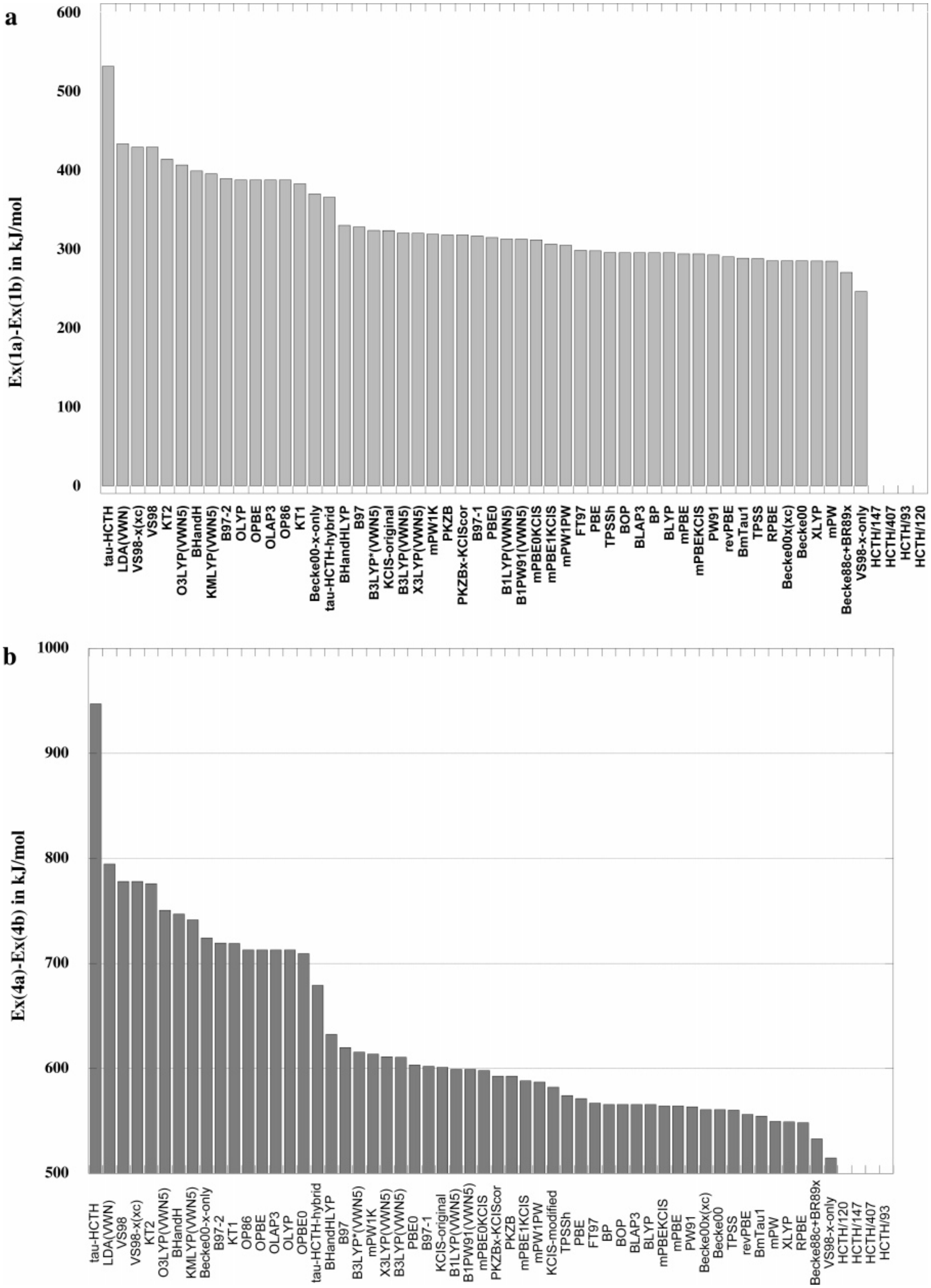

Figure 7. (a) Exchange energy gap between the valence isomers **1a** and **1b**. (b) Exchange energy gap between the valence isomers **4a** and **4b**.

was investigated at various levels of calculation using the 6-311+G* basis set (Table 4). Again, B3PW91 results deviates from B3LYP and MP2 results.

The exchange energy difference ΔEx between **1a** and **1b** (respectively **4a** and **4b**) is about two to three times larger than ΔEc (Figures 7a and 7b) and varies almost continuously in the

TABLE 4: Energy Gap (kJ/mol) between Acyclic and Cyclic Isomers of H_2C_3O, Obtained at Various Levels of Calculation (6-311+G* Basis Set)

method	B3PW91	B3LYP	MP2
propynal	0.0	0.0	0.0
cyclopropenone	0.2	5.0	7.4

TABLE 5: Energy Decomposition Analysis

	C_9O_3/PBE, kJ/mol					
	n-C_3O	*cyc*-C_3O	**1a**	**1b**	*cyc*-C_3O-n-C_3O	**1b**−**1a** *vs* fragments
Pauli repulsion						
kinetic (DT)	27924.9	32539.2	19198.9	12718.2	4614	−6481
DV Pauli Coulomb	−14613.6	−16310.5	−8071.2	−6065.3	−1697	2006
DV Pauli LDA-XC	−3340.2	−3817.4	−3186.8	−2257.9	−477	929
DV Pauli GGA-exchange	−22.4	−26.9	−116.8	−103.0	−5	14
DV Pauli GGA-correlation	139.3	160.0	286.6	241.5	21	−45
total Pauli repulsion	10087.9	12544.4	8110.7	4533.5	2456	−3577
electrostatic interaction	−2126.2	−2713.4	−2889.8	−1620.7	−587	1269
total steric interaction	7961.7	9831.0	5220.9	2912.8	1869	−2308
orbital interactions						
a_1	−6770.7	−7517.4			−747	
a_2	306.4	119.3			−187	
b_1	−1894.1	−2120.7			−227	
b_2	−1713.3	−2987.4			−1274	
a′			−6147.6	−3298.5		2849
a″			−1585.9	−392.4		1193
total orbital interactions	−10071.7	−12506.2	−7733.5	−3691.0	−2435	4043
alternative decomposition orbital interactions						
kinetic	−26502.6	−30712.2	−15284.7	−10042.6	−4210	5242
Coulomb	15028.9	16848.0	7412.9	6010.8	1819	−1402
XC	1402.0	1358.0	138.4	340.9	−44	203
total orbital interactions	−10071.7	−12506.2	−7733.5	−3691.0	−2435	4043
total bonding energy	−2110.0	−2675.2	−2512.6	−778.2	−565	1734

TABLE 6: Summary of the Energy Decomposition Analysis

	C_9O_3/PBE, kJ/mol					
	n-C_3O	*cyc*-C_3O	**1a**	**1b**	*cyc*-C_3 O − *n*-C_3O	**1b** − **1a** *vs* fragments
electrostatic energy	−2126.2	−2713.4	−2889.8	−1620.7	−587	1269
kinetic energy	1422.3	1827.0	3914.2	2675.6	405	−1239
Coulomb (Steric+Orb Int) energy	415.3	537.6	−658.4	−54.6	122	604
XC energy	−1821.3	−2326.4	−2878.6	−1778.5	−505	1100
total bonding energy	−2110.0 *3	−2675.2 *3	−2512.6	−778.2	−565 *3	1734
total bonding energy from atoms	−6329.9	−8025.7	−8842.4	−8803.8	−1695	39

range 550−800 kJ/mol. Replacing partially the GGA exchange by exact exchange tends to increase the value of ΔEx. For example, ΔEx increases through the changes: PBE→PBE0, BLYP→B3LYP, i.e., GGA→HDFT. Similarly, the OPTX exchange favors the polycyclic isomers by 150 kJ/mol as compared to the Becke exchange.

For some properties like bond length alternation in polymers, it has been found that the percentage of exact exchange in the hybrid functional could be important and even the leading term.[45] This is strongly related to the subtle balance between the overestimated localization introduced by the exact (Hartree−Fock-like) exchange and the overestimated delocalization introduced by the LDA/GGA functionals. This feature seems to be relevant in the present systems as well, where the extent of electron delocalization may be different in both valence isomers. Indeed **4** is already a much larger system than **1**−**3**, so that the importance of the localization/delocalization balance is increased, probably giving an increased importance of the exchange counterpart with respect to the (dynamic) correlation: this should also be at the origin of the bent structures of **4a** and **4b** as compared to the planar structures of **1**−**3**. This loss of planarity will, in turn, lead to a decreased importance of the (dynamic) correlation.

With the exception of the τ-HCTH functional and, to a smaller extent, of the VSXC/(VS98) functional, in which huge exchange energy differences are balanced by a large contribution of the correlation counterpart, one can see that the exchange energy differences are generally between two and three times larger than the correlation energy differences. This may rule out the dominant role of the correlation part in the discrepancy of the results deduced from the above analysis of Table 3. Like for compounds **1**−**3**, the OPTX exchange functional and also the Scuseria's VS98 and Tozer's KT functionals overestimate the stabilization of the monocyclic isomer with respect to the other hybrid or (*meta*-) GGA functionals. For the latter, the dispersion of the energy differences is about 50 kJ/mol, to be compared with the 100 kJ/mol difference between the LYP/Lap and other correlation functionals.

7. Energy Decomposition Analysis. In a static approach, cyclic electron delocalization (i.e., aromaticity in the broad sense) within both the central cyclohexatriene unit ("benzene" ring) and the benzannelated cyclopropenone fragments is *a priori* expected to stabilize the tetracyclic structure **1b** with respect to **1a.** However, the relative energy of **1a** and **1b** is a relevant measure of their relative *stability* only if they are connected by an interconversion pathway of sufficiently low barrier. Otherwise, their "chemical existence" may be better compared through their stabilization energy with respect to "natural" fragments (just as the heat of formation of compounds with respect to standard states of the constituting elements, or the complexation free enthalpy of complexes with respect to the corresponding metal ion and free ligands).

For example, the putative oxocarbons are fascinating cyclo-oligomers of carbon monoxide. By analogy, structure **1a** can be regarded as the cyclo-trimer of a linear C_3O fragment, namely the *carbo*-mer of carbon monoxide (Scheme 5). Likewise, structure **1b** is formally the cyclo-trimer of a cyclic C_3O fragment, namely cyclopropynone (Scheme 5). It is well-known that despite its carbenic character, carbon monoxide has no propensity to oligomerize, and the question is open for its *carbo*-

TABLE 7: List of Acronyms of the DFT Functionals Used in This Work and the Corresponding Literature References

XC functional combination	(in most cases a sum of exchange and correlation counterparts, sometimes not dissociated)	ref
hybrid functionals	They derive all from the three-parameter hybrid functional mixing the exact Hartree−Fock exchange with, e.g. the VWN5, B88x, and PW91c functionals first proposed by Becke: Exc = Ex(LDA) + Ec(LDA) + a0 [Ex(HF) - Ex(LDA)] + ax Ex(B88x) + ac Ec(PW91c)	47
B, or B88, or Be88 or B88x	exchange GGA proposed by Becke, in 1988. Widely used, in particular within hybrid combinations. It is an improvement over Becke's 1986 (A and B) exchange functionals.	48
B1LYP(VWN5)	one-parameter hybrid functional $Exc = Exc^{BLYP} + a (Ex^{HF} - Ex^{BLYP})$ a = 0.25	
B1PW91(VWN5)	one-parameter hybrid functional $Exc = Exc^{PW91} + a (Ex^{HF} - Ex^{PW91})$ a = 0.25	
B3LYP(VWN3) B3LYP(VWN5)	The B3LYP functional is a Gaussian (Inc.) variation on Becke's original B3PW91[47] hybrid functional. The functional writes Exc = (1-a0)Ex(LDA) + a0 Ex(HF) + ax Ex(B88x) + ac Ec(LYP88c) + (1-ac) Ec(VWN3) , where a0 = 0.20, ax = 0.72 and ac = 0.81 . See note about VWN3/VWN5.	49
B3LYP*(VWN5)	Idem B3LYP with a0 = 0.15, ax = 0.72 and ac = 0.81	50
B97	original Becke (1997) hybrid GGA : a0 = 0.194	51
B97-1	reparametrizations of B97 : a0 = 0.21	52
B97-2		53
BHandH	Idem B3LYP with a0 = 0.50, ax = 0 and ac = 1	
BHandHLYP	Idem B3LYP with a0 = 0.50, ax = 0.5 and ac = 1	
BLAP3	B88 (exchange) + LAP (correlation) GGA: uses the set of three parameters driving the LAP functional	37
BLYP	B88 (exchange) + LYP (correlation)	54
BOP	B88 (exchange) + Tsuneda et al. OP (correlation)	35
BP or BP86 or B88P86	B88 (exchange) + P86 (correlation)	
Becke00 Becke00-x-only Becke00x(xc)	Becke 2000 *meta-GGA*: exchange and correlation. (original and exchange only)	33
Becke88c+BR89x	Becke-Roussel GGA	55
Bmτ1	modified Be88 for exchange, and Tau1 *meta-GGA* for correlation	38
FT97	Filatov and Thiel's GGA	56
HCTH/93	Hamprecht, Cohen, Tozer and Handy's variations of a *GGA* functional of B97 type parametrized with increasing databases.	52
HCTH/120		57
HCTH/147		
HCTH/407		
KCIS-modified	Krieger, Chen, Iafrate and Kurth modified Krieger−Chen−Iafrate−Savin functional	58
KCIS-original	Krieger−Chen−Iafrate−Savin functional	59
KMLYP(VWN5)	Kang and Musgrave hybrid parametrization	60
KT1 KT2	Keal and Tozer GGA parametrizations	61
LAP	Proynov et al. *meta-GGA* correlation energy functional (the first with Laplacian). To be coupled to B88 or PW86 exchange functionals. Ancestor of τ1 or τ2 functionals.	36
LDAx or S	Dirac−Slater local exchange	62
LDA or LDAc VWN or VWN5	parametrization of the LDA correlation energy by Vosko, Wilk, and Nusair, usually referred to as VWN, also VWN5.	63
LYP or LYP88	Lee, Yang, and Parr GGA correlation functional.	64
OPTX	GGA exchange proposed by Handy and Cohen	65
OLAP3	OPTX (exchange) + LAP3(correlation).	
OLYP	OPTX (exchange) + LYP (correlation).	
OP86	OPTX (exchange) + P86 (correlation).	
OPBE	OPTX (exchange) + PBEc (correlation).	66
OPBE0	hybrid with OPTX (exchange) + PBEc (correlation) and a0 = 0.25	
O3LYP(VWN5)	Exc = (1-a0) Ex(LDA) + a0 Ex(HF) + ax Ex(OPTX) + ac Ec(LYP88c) + (1-ac) Ec(LDA) , where a0 = 0.20, ax = 0.72, and ac = 0.81.	
P86	first Perdew's correlation GGA energy functional.	67
PBE	GGA developed by Perdew, Burke, and Ernzerhof, including two components: PBEx + PBEc	68
PBE0	hybrid functional with PBE and 25% HF exchange, developed by Adamo + Barone and Ernzerhof + Scuseria, also referred to as PBE1PBE	69
PKZB	*meta-GGA* proposed by Perdew, Kurth, Zupan, and Blaha; contains exchange (PKZBx) and correlation (PKZBc) parts.	70
PKZBx-KCIScor	as indicated	
PW91	GGA exchange and correlation functionals developed by Perdew and Wang.	71
	PW91 is a reduced acronym for PW91x + PW91c	72
RPBE	RPBEx: revised PBE exchange proposed in 1999 by Hammer−Hansen−Norskov: RPBE = RPBEx + PBEc.	73
TPSS	Tao, Perdew, Staroverov, and Scuseria *meta-GGA* functional for exchange and correlation	74
TPSSh	hybrid functional with TPSS and 10% of HF exchange	75
VS98 or VSXC	*meta-GGA* derived from a density matrix expansion: 21 fitted parameters.	76
VS98-x(xc), VS98-x-only	variants of VS98 keeping only the X part.	
XLYP	XLYP = (exchange, X = 0.722Becke + 0.347PW91) + LYP (correlation).	77
X3LYP(VWN5)	Exc = (1-a0) Ex(LDA) + a0 Ex(HF) + ax Ex(X) + ac Ec(LYP88c) + (1-ac) Ec(LDA), where a0 = 0.218, ax = 0.542*Ex(Be88) + 0.167*Ex(PW91x) and ac = 0.871.	
mPBE	mPBEx + PBEc	78
	mPBEx: Adamo+Barone's modified PBEx	
mPBE0KCIS	hybrid *meta-GGA* derived from PBE exchange + KCIS correlation, a0 = 0.25	79
mPBE1KCIS	hybrid *meta-GGA* derived from PBE exchange + KCIS correlation, a0 = 0.177	79
mPBEKCIS	*meta-GGA* derived from PBE exchange + KCIS correlation	79

TABLE 7: (Continued)

XC functional combination	(in most cases a sum of exchange and correlation counterparts, sometimes not dissociated)	ref
mPW mPW1PW	mPW: mPWx + PW91c ; mPWx: the modified PW91 exchange correction proposed in 1998 by Adamo and Barone; mPW1PW: hybrid a0 = 0.25;	80
mPW1K	mPW1K: hybrid a0 = 0.428 (supposed to better describe weak interactions)	81
revPBE	Zhang and Yang modification of the PBE parametrization	82
tau-HCTH	*meta-GGA* derived from HCTH by inclusion of kinetic energy density contribution	83
tau-HCTH-hybrid	hybrid variation of HCTH (variable a0)	83
VWN5 or VWN80	see LDA (correlation)	
VWN3	VWN3 is incorporated (apparently by mistake) in the popular B3LYP functional, it is based upon the inaccurate random phase approximation for the electron gas of uniform density, where VWN5 is more sound, based on the homogeneous electron gas data of quantum Monte Carlo simulations by Ceperley and Alder. For the difference between VWN3 and VWN5, see, e.g., Hertwig and Koch.[84]	63

mer C_3O. The formal aromaticity of the triply zwitterionic resonance form of **1a** (six π_z electrons over the C_9 ring) might be a driving force of its existence. The formation of **1a** from *n*-C_3O is also formally allowed by the Dewar−Zimmermann rule (three π bonds, namely six π electrons, are moved while the final σ bonds were pre-existing at the carbene centers). The relative stabilization energy of **1a** and **1b** can thus be appraised through an analysis of the interaction between *n*-C_3O and *cyc*-C_3O fragments, respectively.

Following Baerends et al. energy decomposition analysis scheme,[46] the bonding energy (with respect to spherical atom energies) results from steric contributions (Pauli repulsion + electrostatic interactions between the fragments) and orbital interaction energies. The latter are due to the interactions between the occupied orbitals of one fragment and the empty orbitals of another fragment. The internal polarization of the fragments, i.e., the interactions between the occupied and empty orbitals within a given fragment, also plays a role.

Table 5 lists the energy decomposition analysis, where the geometry of skewed *n*-C_3O (respectively *cyc*-C_3O) fragments has been extracted from the geometry of **1a** (respectively **1b**).

The energy decomposition analysis is first applied to the C_3O fragments. It is clear that the *cyc*-C_3O fragment suffers from a stronger Pauli repulsion with respect to the *n*-C_3O fragment by ca. 2500 kJ/mol. This holds to the deviation of the valence angles of the C atoms involved in the C−O bond, from the pure Csp^2 value of 120°. Indeed, this deviation is larger in *cyc*-C_3O (2 × 151.6°, 56.8°) than in *n*-C_3O (2 × 128.4°, 103.2°). This is mainly due to an increased kinetic energy contribution (difference equal to ca. 4600 kJ/mol), not balanced by the variation of the corresponding Coulomb energies (difference of ca. −1700 kJ/mol), and of the exchange-correlation energies (difference of ca. −400 kJ/mol). It can be henceforth noticed that the exchange-correlation contribution within a GGA functional (here the PBE functional) comes mainly from the correlation term (21 kJ mol^{-1}) rather than from the exchange counterpart (−5 kJ/mol). This is in contrast to the general trend that exchange energies are roughly 1 order of magnitude larger than correlation energies. However, this is in agreement with the fact that these systems differ mainly by the topology of their π-systems, involving a strong dynamic correlation (differences in energies are discussed here). The stronger Pauli repulsion in the *cyc*-C_3O fragment (with respect to the *n*-C_3O fragment) is far from being canceled by electrostatic interactions (difference of ca. 600 kJ/mol). Consequently, the total steric interaction favors the *n*-C_3O fragment by ca. 1900 kJ/mol, but the steric interaction is then overcompensated by the orbital interactions (difference of ca. 2400 kJ/mol in favor of the *cyc*-C_3O fragment). This is due to the π-conjugation and mostly through the orbitals belonging to the irreducible representation b_2. Finally, the *cyc*-C_3O fragment is more stable than the *n*-C_3O fragment by ca. −565 kJ/mol.

The interaction between the C_3O fragments shows the opposite trends. The tetracyclic isomer **1b** suffers from a Pauli repulsion of its constitutive fragments weaker than that occurring in the monocyclic isomer **1a** (difference of ca. 3600 kJ/ mol, with ca. 6500 kJ/mol for the kinetic part, and −2000 kJ/mol for the Coulomb contribution, for the three bonds between the C_3O fragments). After addition of the electrostatic interaction, ca. −1300 kJ/mol in favor of **1a**, tetracyclic **1b** exhibits a steric interaction between its three fragments which is lowered by ca. 2300 kJ/mol. On the other hand, the orbital interactions obviously favor **1a** vs **1b** (difference of ca. 4000 kJ/mol), so that monocyclic C_9O_3 **1a** is finally found to be slightly more *stabilized* than the tetracyclic isomer **1b** by 39 kJ/mol only (Table 6).

Table 6 also shows that the exchange-correlation energy favors each *cyc*-C_3O fragment by ca. −500 kJ/mol, whereas it favors the monocyclic structure **1a** by 1100 kJ/mol. The balance between electrostatic, kinetic energy, and Coulomb (steric + orbital interactions) contributions is thus quite subtle. In other words, it would have been difficult to predict the relative stabilization of the two isomers on the sole basis of qualitative contributions based on formal aromaticity arguments.

Concluding Remarks

The variety of problems in molecular chemistry and other fields that can benefit from the efficiency of DFT is much larger than the usual training or testing sets used in the development of the XC functional. This highlights the fundamental importance of "exotic" cases, where a large variety of different functionals show a broad dispersion of the results. The molecules studied in this paper belong in this category, for which a systematic comparison of the performance of a rather exhaustive set of different functional types was desirable. In the selected isomers of molecules **1**, **2**, and **3**, the planar structure involves a large π system for which the effect of the DFT correlation energy is significantly different, depending on whether it was derived from either the Colle−Salvetti correlation formula or the electron gas. These *carbo*-meric molecules should enter among severe tests that brought the XC functional data bank to its knees, such as—but in a totally different way—the simple H abstraction reaction.

Acknowledgment. The authors thank CALMIP (Calcul intensif en Midi-Pyrénées, Toulouse, France), IDRIS (Institut du Développement et des Ressources en Informatique Scientifique, Orsay, France), and CINES (Centre Informatique de l'Enseignement Supérieur, Montpellier, France) for computing facilities and the Ministère de l'Education Nationale de la Recherche et de la Technologie for ACI financial support. Authors warmly thank Dr. E. Proynov for fruitful discussions and suggestions.

Appendix

A list of acronyms of the DFT functionals used in this work with the corresponding literature references is given in Table 7. A GGA functional is a functional of both the density and the gradient of the density. Furthermore, a *meta*-GGA may include the Laplacian of the density, the kinetic energy density, or both ingredients. Surveys of some of them may be found in ADF user guide (http://www.scm.com), Gaussian03 user guide (http://www.Gaussian.com), and Professor Mark Casida's website (http://www-ledss.ujf-grenoble.fr/PERSONNEL/LEDSS7/casida/ CompChem/DFT.html).

Supporting Information Available: Comparison of the calculated geometry (D_{3h} symmetry) and the electronic structure of **1a** (respectively **1b**) at various calculation levels (6-311+G* basis set): Table S1 (respectively S2). Comparison of the frontier orbitals of **1a** (respectively **1b**) at various levels of calculations: Figures S1a (respectively S1b). Cartesian coordinates, total electronic energies in atomic units, and symmetry of structures **1**−**4** computed at the B3PW91/6-311+G** level. Tables of values used for the drawing of Figures 2 and 3 and Figures 5−7. This material is available free of charge via the Internet at http://pubs.acs.org.

References and Notes

(1) Chauvin, R. *Tetrahedron Lett.* **1995**, *36*, 397.

(2) Chauvin, R.; Lepetit, C. *Acetylene Chemistry. Chemistry, Biology and Material Sciences*; Diederich, F.; Stang, P. J., Tykwinski, R. R., Eds.; Wiley: Weinheim, 2005; Chapt. 1, p 1.

(3) Lepetit, C.; Silvi, B.; Chauvin, R. *J. Phys. Chem. A* **2003**, *107*, 464.

(4) (a) Godard, C.; Lepetit, C.; Chauvin, R. *Chem. Commun.* **2000**, 1833. (b) Lepetit, C.; Godard, C.; Chauvin, R. *New J. Chem.* **2001**, *25*, 572.

(5) Lepetit, C.; Peyrou, V.; Chauvin, R. *Phys. Chem. Chem. Phys.* **2004**, *6*, 303.

(6) Lepetit, C.; Nielsen, M. B.; Diederich, F.; Chauvin, R. *Chem. Eur. J.* **2003**, *9*, 5056.

(7) (a) Ducere, J. -M.; Lepetit, C.; Lacroix, P. G.; Heully, J.-L.; Chauvin, R. *Chem. Mater.* **2002**, *14*, 3332. (b) Lepetit, C.; Lacroix, P. G.; Peyrou, V.; Saccavini, C.; Chauvin, R. *J. Comput. Methods Sci. Eng.* **2004**, *4* (3−4), p 569.

(8) (a) Kuwatani, Y.; Watanabe, N.; Ueda, I. *Tetrahedron Lett.* **1995**, *36*, 119. (b) Chauvin, R. *Tetrahedron Lett.* **1995**, *36*, 397. (c) Suzuki, R.; Tsukude, H.; Watanabe, N.; Kuwatani, Y.; Ueda, I. *Tetrahedron* **1998**, *54*, 2477. (d) Maurette, L.; Tedeschi, C.; Sermot, E.; Soleilhavoup, M.; Hussain, F.; Donnadieu, B.; Chauvin, R. *Tetrahedron* **2004**, *60*, 10077. (e) Zou, C.; Lepetit, C.; Coppel, Y.; Chauvin, R. *Pure Appl. Chem.* **2006**, *78*, 791. (f) Maraval, V.; Chauvin, R. *Chem. Rev.*, in press. (g) Saccavini, C.; Tedeschi, C.; Maurette, L.; Sui-Seng, C.; Zou, C.; Soleilhavoup, M.; Vendier, L.; Chauvin, R. *Chem. Eur. J.*, in press. (h) Saccavini, C.; Sui-Seng, C.; Maurette, L.; Lepetit, C.; Soula, S.; Zou, C.; Donnadieu, B.; Chauvin, R. *Chem. Eur. J.*, in press.

(9) Serratosa, F. *Acc. Chem. Res.* **1983**, *16*, 170.

(10) Gicquel, M.; Lepetit, C.; Heully, J.-L.; Chauvin, R. *Chimia* **2005**, *59*, 448.

(11) Gicquel, M.; Heully, J.-L.; Lepetit, C.; Chauvin, R. To be published.

(12) (a) Jemmis, D. E.; Kiran, B. *J. Org. Chem.* **1996**, *61*, 9006. (b) Baldridge, K. K.; Siegel, J. S. *J. Am. Chem. Soc.* **1992**, *114*, 9583. (c) Apeloig, Y.; Karni, M.; Arad, D. In *Strain and Its Implications in Organic Chemistry*; de Meijere, A., Blechert, S., Eds.; Kluwer Academic Publishers: Dordrecht, The Netherlands, 1989; pp 457−462. (d) Apeloig, Y.; Arad, D.; Halton, B.; Lifford, C.; Randall, J. *J. Am. Chem. Soc.* **1986**, *108*, 3241.

(13) Frisch, M. J.; Trucks, G. W.; Schlegel, H. B.; Scuseria, G. E.; Robb, M. A.; Cheeseman, J. R.; Montgomery, J. A., Jr.; Vreven, T.; Kudin, K. N.; Burant, J. C.; Millam, J. M.; Iyengar, S. S. Tomasi, J.; Barone, V.; Mennucci, B.; Cossi, M.; Scalmani, G.; Rega, N.; Petersson, G. A.; Nakatsuji, H.; Hada, M.; Ehara, M.; Toyota, K.; Fukuda, R.; Hasegawa, J.; Ishida, M.; Nakajima, T.; Honda, Y.; Kitao, O.; Nakai, H.; Klene, M.; Li, X.; Knox, J. E.; Hratchian, H. P.; Cross, J. B.; Adamo, C.; Jaramillo, J.; Gomperts, R.; Stratmann, R. E.; Yazyev, O.; Austin, A. J.; Cammi, R.; Pomelli, C.; Ochterski, J. W.; Ayala, P. Y.; Morokuma, K.; Voth, G. A.; Salvador, P.; Dannenberg, J. J.; Zakrzewski, V. G.; Dapprich, S.; Daniels, A. D.; Strain, M. C.; Farkas, O.; Malick, D. K.; Rabuck, A. D.; Raghavachari, K.; Foresman, J. B.; Ortiz, J. V.; Cui, Q.; Baboul, A. G.; Clifford, S.; Cioslowski, J.; Stefanov, B. B.; Liu, G.; Liashenko, A.; Piskorz, P.; Komaromi, I.; Martin, R. L.; Fox, D. J.; Keith, T.; Al-Laham, M. A.; Peng, C. Y.; Nanayakkara, A.; Challacombe, M.; Gill, P. M. W.; Johnson, B. W.; Wong, W.; Gonzalez, C. and Pople, J. A., *Gaussian 03*, *Revision B.05*, Gaussian, Inc., Pittsburgh PA, 2003.

(14) Baerends, E. J.; Autschbach, J.; Bérces, A.; Bo, C.; Boerrigter, P. M.; Cavallo, L.; Chong, D. P.; Deng, L.; Dickson, R. M.; Ellis, D. E.; Fan, L.; Fischer, T. H.; Fonseca Guerra, C.; van Gisbergen, S. J. A.; Groeneveld, J. A.; Gritsenko, O. V.; Grüning, M.; Harris, F. E.; van den Hoek, P.; Jacobsen, H.; van Kessel, G.; Kootstra, F.; van Lenthe, E.; McCormack, D. A.; Osinga, V. P.; Patchkovskii, S.; Philipsen, P. H. T.; Post, D.; Pye, C. C.; Ravenek, W.; Ros, P.; Schipper, P. R. T.; Schreckenbach, G.; Snijders, J. G.; Sola, M.; Swart, M.; Swerhone, D.; te Velde, G.; Vernooijs, P.; Versluis, L.; Visser, O.; van Wezenbeek, E.; Wiesenekker, G.; Wolff, S. K.; Woo, T. K.; Ziegler, T. ADF2005.01, SCM; Theoretical Chemistry, Vrije Universiteit: Amsterdam, The Netherlands, http://www.scm.com.

(15) Molekel 4.3 by Stefan Portmann and Peter, F. Flükiger, H. P. Lüthi, J. Weber, at University of Geneva and Swiss Center for Scientific Computing, Manno, Switzerland, 2002. www.cscs.ch/molekel.

(16) Straatsma, T. P.; Apra, E.; Windus, T. L.; Bylaska, E. J.; de Jong, W.; Hirata, S.; Valiev, M.; Hackler, M. T.; Pollack, L.; Harrison, R. J.; Dupuis, M.; Smith, D. M. A.; Nieplocha, J.; Tipparaju, V.; Krishnan, M.; Auer, A. A.; Brown, E.; Cisneros, G.; Fann, G. I.; Fruchtl, H.; Garza, J.; Hirao, K.; Kendall, R.; Nichols, J. A.; Tsemekhman, K.; Wolinski, K.; Anchell, J.; Bernholdt, D.; Borowski, P.; Clark, T.; Clerc, D.; Dachsel, H.; Deegan, M.; Dyall, K.; Elwood, D.; Glendening, E.; Gutowski, M.; Hess, A.; Jaffe, J.; Johnson, B.; Ju, J.; Kobayashi, R.; Kutteh, R.; Lin, Z.; Littlefield, R.; Long, X.; Meng, B.; Nakajima, T.; Niu, S.; Rosing, M.; Sandrone, G.; Stave, M.; Taylor, H.; Thomas, G.; van Lenthe, J.; Wong, A.; Zhang, Z. *NWChem, A Computational Chemistry Package for Parallel Computers, Version 4.6*; Pacific Northwest National Laboratory: Richland, WA, 2004.

(17) (a) Schmidt, M. W.; Baldridge, K. K.; Boatz, J. A.; Elbert, S. T.; Gordon, M. S.; Jensen, J. H.; Koseki, S.; Matsunaga, N.; Nguyen, K. A.; Su, S. J.; Windus, T. L.; Dupuis, M.; Montgomery, J. A. *J. Comput. Chem.* **1993**, *14*, 1347−1363. (b) Advances in electronic structure theory: GAMESS a decade later. Gordon, M. S.; Schmidt, M. W. In *Theory and Applications of Computational Chemistry, the First Forty Years*; Dykstra, C. E., Frenking, G., Kim, K. S., Scuseria, G. E., Eds.; Elsevier: Amsterdam, 2005. http://www.msg.ameslab.gov/GAMESS/GAMESS.html.

(18) (a) Sui-Seng, C.; Soleilhavoup, M.; Maurette, L.; Tedeschi, C.; Donnadieu, B.; Chauvin, R. *Eur. J. Org. Chem.* **2003**, 1641. (b) Li, M.; Zou, C.; Duhayon, C.; Chauvin, R. *Tetrahedron Lett.* **2006**, *47*, 1047.

(19) Sakai, S. *J. Phys. Chem. A* **2002**, *67*, 11526.

(20) Stowasser, R.; Hoffmann, R. *J. Am. Chem. Soc.* **1999**, *121*, 3414.

(21) Koch, W.; Holthausen, M. C. *A Chemist's Guide to Density Functional Theory*; Wiley-VCH: New York, 2000.

(22) (a) Plattner, D. A.; Houk, K. N. *J. Am. Chem. Soc.* **1995**, *117*, 4405. (b) Pomerantz, A. E.; Han, J. H.; Musgrave, C. B. *J. Phys. Chem. A* **2004**, *108*, 4030.

(23) Lee, T. J.; Taylor, P. R. *Int. J. Quant. Chem. Symp.* **1989**, *23*, 199.

(24) See, e.g.: (a) Schipper, P. R. T.; Gritsenko, O. V.; Baerends, E. J. *Phys. Rev. A* **1998**, *57*, 1729. (b) Gritsenko, O. V.; Ensing, B.; Schipper, P. R. T.; Baerends, E. J. *J. Phys. Chem. A* **2000**, *104*, 8558. (c) Gritsenko, O. V.; Schipper, P. R. T.; Baerends, E. J. *J. Chem. Phys.* **1997**, *107*, 5007. (d) Chermette, H.; Ciofini, I.; Mariotti, F.; Daul, C. *J. Chem. Phys.* **2001**, *114*, 1447. (e) Becke, A. D. *J. Chem. Phys.* **1996**, *104*, 1040.

(25) Handy, N. C.; Cohen, A. J. *Mol. Phys.* **2001**, *99*, 403.

(26) Chermette, H. *New J. Chem.* **1982**, *16*, 1081.

(27) Baerends, E. J.; Ellis, D. E.; Ros, P. *Chem. Phys.* **1973**, *2*, 41.

(28) Grüning, M.; Gritsenko, O. V.; Baerends, E. J. *J. Phys. Chem. A* **2004**, *108*, 4459.

(29) Zein, S.; Borshch, S. A.; Fleurat-Lessard, P.; Casida, M. E.; Chermette, H. *J. Chem. Phys.*, in press.

(30) Voorhis, T. V.; Scuseria, G. E. *J. Chem. Phys.* **1998**, *109*, 400.

(31) Curtiss, L. A.; Raghavachari, K.; Tracks, G. W.; Pople, J. A. *J. Chem. Phys.* **1991**, *94*, 7221.

(32) Sancho-García, J. C.; Cornil, J. *J. Chem. Phys.* **2004**, *121*, 3096.

(33) Becke, A. D. *J. Chem. Phys.* **2000**, *112*, 4020.

(34) Colle, R.; Salvetti, D. *Theor. Chim. Acta* **1975**, *37*, 329.

(35) Tsuneda, T.; Suzumura, T.; Hirao, K. *J. Chem. Phys.* **1999**, *110*, 10664.

(36) Proynov, E. I.; Vela, A.; Salahub, D. R. *Chem. Phys. Lett.* **1994**, *230*, 419. Erratum, *Chem. Phys. Lett.* **1995**, *234*, 462.

(37) Proynov, E. I.; Ruiz, E.; Vela, A.; Salahub, D. R. *Int. J. Quant. Chem. Symp.* **1995**, *29*, 61.

(38) Proynov, E. I.; Chermette, H.; Salahub, D. R. *J. Chem. Phys.* **2000**, *113*, 10113.

(39) Sancho-Garcia, J. C. *J. Chem. Phys.* **1997**, *124*, 124112.

(40) Becke, A. D. *J. Chem. Phys.* **1997**, *107*, 8554.

(41) Ciofini, I.; Chermette, H.; Adamo, C. *Chem. Phys. Lett.* **2003**, *380*, 12.

(42) Ciofini, I.; Adamo, C.; Chermette, H. *Chem. Phys.* **2005**, *309*, 67.

(43) Ciofini, I.; Adamo, C.; Chermette, H. *J. Chem. Phys.* **2005**, *123*, 121102.

(44) (a) von R. Schleyer, P.; Jiao, H.; Sulzbach, H. M.; Schaeffer, H. F., III. *J. Am. Chem. Soc.* **1996**, *118*, 2093. (b) Sulzbach, H. M.; Schaeffer, H. F., III. *J. Am. Chem. Soc.* **1996**, *118*, 3519. (c) Jemmis, E. D.; Kiran, B. *J. Org. Chem.* **1996**, *61*, 9006. (d) Xie, Y.; Schaeffer, H. F., III; Liang, G.; Bowen, J. P. *J. Am. Chem. Soc.* **1994**, *116*, 1442. (e) Farnell, L.; Kao, J.; Schaeffer, H. F., III. *J. Am. Chem. Soc.* **1981**, *103*, 2148.

(45) Jacquemin, D.; Perpète, E. A.; Ciofini, I.; Adamo, C. *Chem. Phys. Lett.* **2005**, *405*, 376.

(46) (a) Bickelhaupt, F. M.; Nibbering, N. M.; van Wezenbeek, E. M.; Baerends, E. J. *J. Phys. Chem.* **1992**, *96*, 4864. (b) Bickelhaupt, F. M.; Baerends, E. J. *Rev. Comput. Chem.* **2000**, *15*, 1. (c) Baerends, E. J. *Cluster Models for Surface and Bulk Phenomena*; Nato Asi Series B; Pacchioni, G.; Bagus, P. S.; Parmigiani, F., Eds.; 1992; Vol. 283, p 189.

(47) Becke, A. D. *J. Chem. Phys.* **1993**, *98*, 5648.

(48) Becke, A. D. *Phys. Rev. A* **1988**, *38*, 3098.

(49) The original published description is apparently that in *Gaussian News* **1994**, *5* (2).

(50) (a) Reiher, M.; Salomon, O.; Hess, B. A. *Theor. Chem. Acc.* **2001**, *107*, 48. (b) Reiher, M. *Inorg. Chem.* **2002**, *41*, 6928.

(51) Becke, A. D. *J. Chem. Phys.* **1997**, *107*, 8554.

(52) Hamprecht, F. A.; Cohen, A. J.; Tozer, D. J.; Handy, N. C. *J. Chem. Phys.* **1998**, *109*, 6264.

(53) Wilson, P. J.; Bradley, T. J.; Tozer, D. J. *J. Chem. Phys.* **2001**, *115*, 9233.

(54) (a) Johnson, B. G.; Gill, P. M. W.; Pople, J. A. *J. Chem. Phys.* **1993**, *98*, 5612. (b) Russo, T. V.; Martin, R. L.; Hay, P. J. *J. Chem. Phys.* **1994**, *101*, 7729.

(55) (a) Becke, A. D.; Roussel, M. R. *Phys. Rev. A* **1989**, *39*, 3761. (b) Becke, A. D. *J. Chem. Phys.* **1988**, *88*, 1053. (c) Becke, A. D. *Int. J. Quant. Chem. Symp.* **1994**, *28*, 625.

(56) Filatov, M.; Thiel, W. *Mol. Phys.* **1997**, *91*, 847.

(57) (a) Boese, A. D.; Doltsinis, N. L.; Handy, N. C.; Sprik, M. *J. Chem. Phys.* **2000**, *112*, 1670. (b) Boese, A. D.; Handy, N. C. *J. Chem. Phys.* **2001**, *114*, 5497.

(58) Krieger, J. B.; Chen, J.; Iafrate, G. J.; Kurth, S. Modified Krieger−Chen−Iafrate−Savin functional. Unpublished.

(59) Krieger, J. B.; Chen, J.; Iafrate, G. J.; Savin, A. In *Electron Correlations and Materials Properties*; Gonis, A., Kioussis, N., Eds.; Plenum: New York, 1999 (original Krieger−Chen−Iafrate−Savin functional).

(60) Kang, J. K.; Musgrave, C. B. *J. Chem. Phys.* **2001**, *115*, 11040.

(61) Keal, T. W.; Tozer, D. J. *J. Chem. Phys.* **2003**, *119*, 3015.

(62) Slater, J. C. *Phys. Rev.* **1951**, *81*, 385.

(63) Vosko, S. H.; Wilk, L.; Nusair, M. *Can. J. Phys.* **1980**, *58*, 1200.

(64) Lee, C.; Yang, W.; Parr, R. G. *Phys. Rev. B* **1988**, *37*, 785.

(65) Handy, N. C.; Cohen, A. J. *Mol. Phys.* **2001**, *99*, 403.

(66) Swart, M.; Ehlers, A. W.; Lammertsma, K. *Mol. Phys.* **2004**, *102*, 2467.

(67) Perdew, J. P. *Phys. Rev. B* **1986**, *33*, 8822. Erratum: *Phys.* Rev. *B* **1986**, *34*, 7406.

(68) Perdew, J. P.; Burke, K.; Ernzerhof, M. *Phys. Rev. Lett.* **1996**, *77*, 3865. Erratum: *Phys. Rev. Lett.* **1997**, *78*, 1386.

(69) (a) Adamo, C.; Barone, V. *J. Chem. Phys.* **1999**, *110*, 6158. (b) Ernzerhof, M.; Scuseria, G. E. *J. Chem. Phys.* **1999**, *110*, 5029.

(70) Perdew, J. P.; Kurth, S.; Zupan, A.; Blaha, P. *Phys. Rev. Lett.* **1999**, *82*, 2544. Erratum *Phys. Rev. Lett.* **1999**, *82*, 5179.

(71) Perdew, J. P.; Chevary, J. A.; Vosko, S. H.; Jackson, K. A.; Pederson, M. R.; Singh, D. J.; Fiolhais, C. *Phys. Rev. B* **1992**, *46*, 6671. Erratum, *Phys. Rev. B* **1993**, *48*, 4978.

(72) Perdew, J. P.; Burke, K.; Wang, Y. *Phys. Rev. B* **1996**, *54*, 16533. Erratum, *Phys. Rev. B* **1998**, *57*, 14999.

(73) Hammer, B.; Hansen, L. B.; Norskov, J. K. *Phys. Rev. B* **1999**, *59*, 7413.

(74) (a) Tao, J.; Perdew, J. P.; Staroverov, V. N.; Scuseria, G. E. *Phys. Rev. Lett.* **2003**, *91*, 146401. (b) Perdew, J. P.; Tao, J.; Staroverov, V. N.; Scuseria, G. E. *J. Chem. Phys.* **2004**, *120*, 6898.

(75) Staroverov, V. N.; Scuseria, G. E.; Tao, J.; Perdew, J. P. *J. Chem. Phys.* **2003**, *119*, 12129.

(76) Voorhis, T. V.; Scuseria, G. E. *J. Chem. Phys.* **1998**, *109*, 400.

(77) Xu, X.; Goddard, W. A., III. *Proc. Nat. Acad. Sci.* **2004**, *101*, 2673.

(78) Adamo, C.; Barone, V. *J. Chem. Phys.* **1996**, *116*, 5933.

(79) Toulouse, J.; Adamo, C. *Chem. Phys. Lett.* **2002**, *362*, 72.

(80) Adamo, C.; Barone, V. *J. Chem. Phys.* **1998**, *108*, 664.

(81) Lynch, B. J.; Fast, P. L.; Harris, M.; Truhlar, D. G. *J. Phys. Chem. A* **2000**, *104*, 4811.

(82) Zhang, Y.; Yang, W. *Phys. Rev. Lett.* **1998**, *80*, 890.

(83) Boese, A. D.; Handy, N. C. *J. Chem. Phys.* **2002**, *116*, 9559.

(84) Hertwig, R. H.; Koch, W. *Chem. Phys. Lett.* **1997**, *268*, 345.